LARGE LOW-ALBEDO ASTEROIDS: DYNAMICAL AND THERMAL CONTEXT. D. Takir[1], W. Neumann[2,3] S.N. Raymond[4], J.P. Emery[5], M. Trieloff[3]. [1]Jacobs, NASA Johnson Space Center, Houston (driss.takir@nasa.gov), TX 77058, USA, [2]German Aerospace Center, Institute of Planetary Research, Berlin, Germany, [2]Institut für Geowissenschaften, Universität Heidelberg, 69120 Heidelberg, Germany. [4]Laboratoire d'Astrophysique de Bordeaux, Pessac, France, [5]Northern Arizona University, Flagstaff, AZ 86011, USA.

Introduction: Low-albedo asteroids, most of which are located in the outer belt and Jupiter's Trojan clouds, provide information related to the origin and evolution of the solar system and the conditions in which the solar nebula was formed. These asteroids are widely thought to be the source of the primitive carbonaceous chondrites and allow us to put crucial constraints on the current dynamical and thermal theories of the formation and evolution of the early solar system.

The nature of surface composition of large and low-albedo asteroids, like (1) Ceres, (10) Hygiea and (52) Europa, is still under intense debate and different interpretations have been put forth to explain the absorption features in these objects (e.g., [1, 2, 3, 4, 5, 6]). Laboratory and spectroscopic experiments on meteorites that represent all nine carbonaceous chondrite types found no spectral matches for these large asteroids (e.g., [7]).

Previous studies of asteroid Ceres (the largest low-albedo asteroid in the solar system) have been conducted to constrain and estimate its surface composition. Using linear mixing, [2] found hydroxide brucite, serpentines, and carbonates, to be consistent with Ceres' ground-based spectra. [5] estimated the surface composition of Ceres and found evidence of widespread NH3-phyllosilicates across its surface using best-fit solutions to Dawn's NIR spectra. The presence of NH3-phyllosilicates implies that material from the outer solar system was incorporated into large low-albedo asteroids, either during their formation at great heliocentric distance or by incorporation of material transported into the Main Belt region [5].

Here we present near-infrared measurements of new large and low-albedo asteroids that share the same spectral similarities with the largest asteroid in the solar system, Ceres. We also present the context of these new observations in terms of their dynamical and thermal origin and evolution.

Orbital distribution and dynamical modeling of large low-albedo asteroids: The orbital distribution of large low-albedo asteroids in Fig. 1 was shaped by the giant planets' growth and migration (see [8]). One implantation mechanism was a simple byproduct of Jupiter's growth, which is thought to have involved the growth of a 10-20 Earth-mass core followed by the slow accumulation of gas and, when the conditions were met, a rapid phase of runaway gas accretion [9, 10]. Jupiter's rapid increase in mass destabilized the orbits of nearby planetesimals and gravitationally scattered them in all directions. Under the action of gas drag, a fraction of planetesimals was implanted onto stable orbits, preferentially in the outer main belt ([11], [12]). This same process was repeated during Saturn's rapid gas accretion. Primitive planetesimals were likely implanted from across the outer solar system and in multiple episodes (Fig. 2). The narrowest possible source region assuming that Jupiter and Saturn grew in-situ with no migration – is still ~5 AU wide, extending from roughly 4-9 AU [11].

Thermal modeling and evolution of low-albedo asteroids: Low-albedo asteroids are thought to be originally composed of mixtures of anhydrous materials and water ice that was later melted by heat sources such as the decay of ^{26}Al, reacting with anhydrous materials to form H_2O/OH-rich minerals [13]. Calculations of the evolution of the temperature and bulk density of initially water-rich small bodies were performed using a 1D finite differences thermal evolution model [14, 15] for ^{26}Al-heated planetesimals. In particular, thermally activated compaction due to hot pressing of bodies with an initially unconsolidated porous structure was modeled for fitting the bulk densities of large low-albedo asteroids under consideration. An ice-rich initial composition that leads to a material dominated by phyllosilicates after aqueous alteration (with ≈13 wt.% H_2O initially that is consumed completely for the aqueous alteration leading to a composition with ≈60 vol.% hydrated silicates) was assumed. A typical initial porosity of 50% [16] is reduced following the change of the strain rate that is calculated as Voigt approximation from the strain rates of components[17]. Material properties (thermal conductivity, density, heat capacity, etc.) correspond to the composition assumed and are adjusted with temperature and porosity. Both short- and long-lived radionuclides are considered as heat sources. Fig. 3 shows the maximum temperature (a) and the average density (b) calculated as functions of diameter and accretion time, as well as the accretion times for several of the asteroids studied that result from the bulk density fits.

The heating and compaction of planetesimals is determined by the availability of ^{26}Al, i.e., by the accretion time t_0 relative to the formation of calcium-aluminum-rich inclusions (CAIs), such that maximum temperatures and structures vary strongly for $t_0 < 3$ Myr rel. to CAIs. However, for a later accretion only

the size of the body determines its maximum temperature and density due to the nearly constant heating by long-lived radionuclides. Average densities of Ceres- and Europa-like group members imply highly porous interiors and, consequently, relatively late accretion at t_0 of 1.5-3.5 Myr rel. to CAIs with a maximum temperature of < 900 K (Fig. 3).

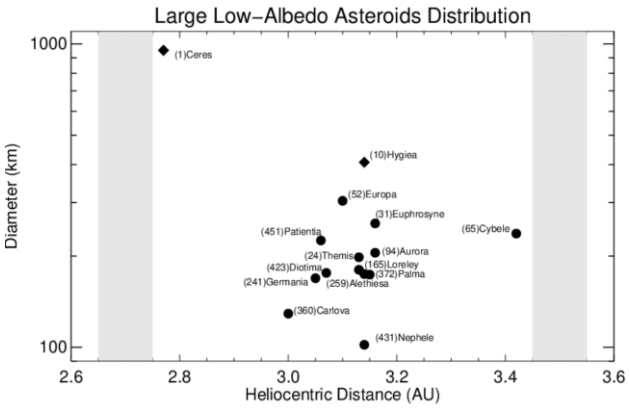

Fig. 1. Orbital distribution of large low-labedo asteroids included in this study. The black diamonds represent Ceres-like group.

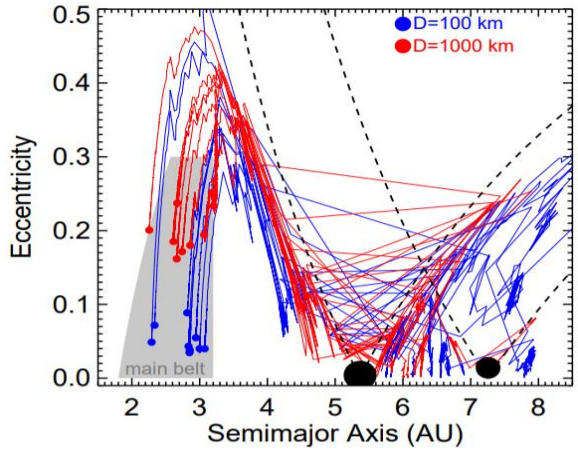

Fig. 2. Implantation of large planetesimals into the asteroid belt during the accretion of the gas giants. Planetesimals were selected from simulations of [11] in which the gas giants started as cores and underwent runaway gas accretion. The dashed curves show orbits that cross those of the growing Jupiter (at 5.4 AU) and Saturn (at 7.25 AU), locked in 3:2 orbital resonance. Planetesimals were scattered by the gas giants onto eccentric orbits in the inner Solar System. Under the action of aerodynamic gas drag the planetesimals' eccentricities dropped sufficiently to be stabilized, preferentially in the outer parts of the main belt. The source region of implanted asteroids in these simulations stretched from 4 to 9 AU.

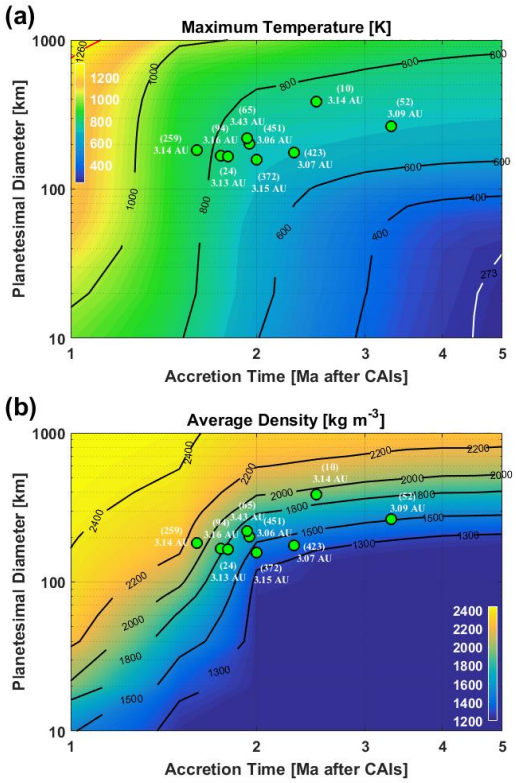

Fig. 3. Maximum temperature (a) and density (b) for initially water-rich planetesimals as functions of the accretion time rel. to CAIs and of the reference diameter. Green dots show some of the studied asteroids with their reference diameters and with accretion times that result from the bulk density fits. Note that a reference diameter corresponds to an object of equal mass with zero porosity, while the actual diameters calculated are larger due to higher bulk porosity values. The studied asteroids' numbers and semi-major axes are also included in the plot.

References: [1] King T.V.V. et al. (1992) *Science* 255, 1551-1553. [2] Miliken R.E. and Rivkin A.S. (2009) *Nat. Geosci.* 2, 258–261. [3] Rivkin, A.S., Emery, J.P.(2010). *Nature* 64, 1322–1323. [4] Takir D. and Emery J.P. (2012) *Icarus*, 219, 641-654. [5] De Sanctis M.C. et al. (2015) *Nature* 528, 241-244. [6] Ammannito E. et al. (2016) *Science* 353, 6303 . [7] Takir et al. (2019) *Icarus*, 333, 243-251. [8] Raymond & Nesvorny (2021) *Cambridge U. Press, Editors : S. Marchi et al.* [9] Pollack, J.B. et al (1996) *Icarus*, Volume 124, Issue 1, pp. 62-85. [10] Ida S. & Lin D.N.C. (2004) AJ 626:1045-1060. [11] Raymond, S. & Izodoro (2017) *Icarus* 297, 134-148. [12] Ronnet, T. et al. (2016) ApJ, 828,109. [13] Grimm, R.E., & McSween, Y.H. (1993) Science 259, 653-655. [14] Neumann W. et al. (2020) *A&A*, A&A 633, A117. 15] Neumann W. et al. (2021) *Icarus*. [16] Henke et al. (2012) A&A, 537, A45. [17] Dygert N. et al. (2016) GRL, 43, 532.